Chapter 12

Optical Coherence Tomography

Authors: Lennart Husvogt, Stefan Ploner, and Andreas Maier

OCT is an interferometry based three-dimensional imaging modality that can be used on scattering media, including several types of body tissues. It provides physicians with in-situ image data in micrometer resolution within seconds. OCT's working principle is similar to ultrasound but uses light instead of sound waves and is also free of potentially harmful ionizing radiation while being non-invasive.

OCT in ophthalmology (the branch of medicine concerned with the eyes) has been pioneered by David Huang, Eric Swanson, and James G. Fujimoto and has since become a standard modality and is widely used by clinicians on a daily basis. Since then, OCT has been continuously developed further, providing significant increases in imaging speed and resolution.

12.1 Working Principle of OCT

OCT uses low-coherence interferometry to determine depth and reflectivity within scattering tissues. In order to understand this process, we recall some basic properties of light and waves from the previous chapters.

A. Maier et al. (Eds.): Medical Imaging Systems, LNCS 11111, pp. 251–261, 2018.
https://doi.org/10.1007/978-3-319-96520-8_12

Figure 12.1: Patient being imaged with a commercial OCT device. Image courtesy of Carl Zeiss Meditec AG.

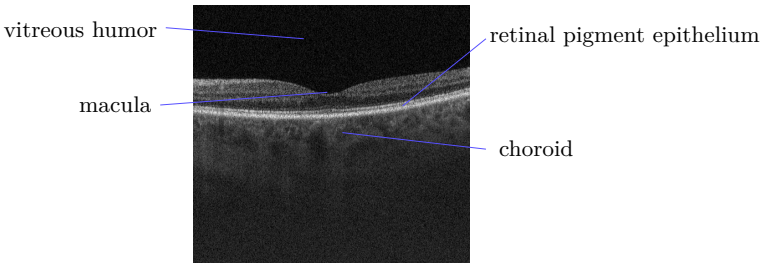

Figure 12.2: OCT B-scan of the retina. Brighter pixels indicate tissue which reflects more light. The upper portion of the figure shows the vitreous humor which has very low reflectivity. The small pit in the center is the macula, the center of vision with the highest resolution. The lowest horizontal bright band corresponds to the retinal pigment epithelium and the cloud-like structure below depicts the choroid, a blood vessel network supplying the retina with nutrients and oxygen.

- Light exhibits properties of particles and waves of which only the latter are relevant for this chapter. Light's electromagnetic wave properties form the basis for OCT.
- Coherence: two waves (or their sources) are described as being coherent with each other, when they have matching wavelengths and the same shift in phase.
- Interference: coherent waves superpose with each other (superposition principle) and can cancel each other out (destructive interference) or reinforce each other (constructive interference).
- Bandwidth describes the width of the spectrum that a light source emits. In contrast, a light source which is monochromatic, only emits light with one wavelength. Such a light source has a bandwidth of 0.

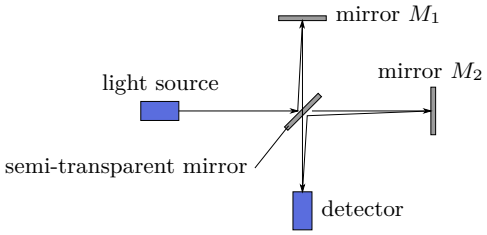

Figure 12.3: Michelson interferometer. Half of the light from the light source travels to mirrors M_1 and M_2 each, before arriving at the detector. Differences in path lengths lead to interference.

12.1.1 Michelson Interferometer

To observe interference of light, interferometers are used. Fig. 12.3 shows a Michelson interferometer. It splits light, coming from a source, into two different paths, where the light can be treated differently, and merges the light, coming back from these two paths, to create interference. Light is split at the semi-transparent mirror in the center and half of it is reflected towards mirror M_1 while the other half passes through the semi-transparent mirror towards mirror M_2. Mirror M_1 reflects the light back towards the semi-transparent mirror where half of the light passes through to a detector. Half of the light coming from mirror M_2 is reflected by the semi-transparent mirror and also travels to the detector. Interference occurs along the distance between the central semi-transparent mirror and the detector. The distance that light travels is called path length and the two paths that the light takes are called arms. If the distances between the semi-transparent mirror and the mirrors M_1 and M_2 are equal, the path lengths are equal and constructive interference will occur.

The detector does not directly detect the waves that form the electromagnetic field, but it detects the intensity of the light, averaged over a small time span, with the detected intensity I being the square of the electromagnetic field E

$$I = E^2. \tag{12.1}$$

12.1.2 Coherence Length

In practice, interference is limited by the coherence length. The coherence length describes how big the difference in path lengths can be for interference to occur. Is the difference in path lengths greater than the coherence length, no interference can be observed. Coherence length is inversely proportional

Geek Box 12.1: Coherence Length

The coherence length l_c of a light source is calculated by

$$l_c = \frac{2 \ln 2}{\pi} \frac{\lambda_0^2}{\Delta\lambda} \tag{12.2}$$

with λ_0 being the central wavelength of the light source and $\Delta\lambda$ its bandwidth. As can be seen, a higher bandwidth leads to a smaller coherence length.

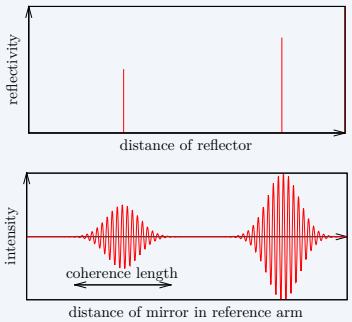

The upper half of the plot shows two reflectors with different reflectivities at different distances (as Dirac impulses). If the reference mirror is moved to match the path length of the reflectors, the measured intensity becomes maximal. Lower coherence lengths also increase resolution.

to the bandwidth (see Geek Box 12.1 for more details on coherence length). Now, if the Michelson interferometer uses a low-coherence light source (a light source which emits a spectrum), the coherence length can be used to determine the distance of a reflector in one of the interferometer's arms by gradually moving the mirror in the other arm. Fig. 12.4 illustrates this, where by moving mirror M_1 to match the distances z_{M_1} and z_{M_2}, will generate an intensity peak in the detector. The plot in Geek Box 12.1 shows how the intensity peaks when z_{M_1} and z_{M_2} are matched.

12.2 Time Domain OCT

The principle of low-coherence interferometry is used by OCT to image scattering samples. The Michelson interferometer is adapted replacing one mirror (M_2 in this case) with a sample (e. g. a patient's eye) to be imaged (cf.

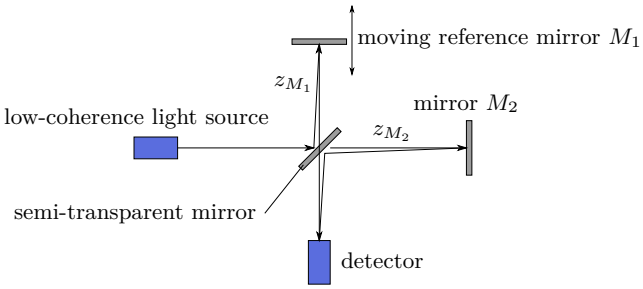

Figure 12.4: Michelson interferometer with low-coherence light source to measure the distance z_{M_2}. Mirror M_1 is moved to match the distances z_{M_1} and z_{M_2} which will generate an intensity peak in the detector.

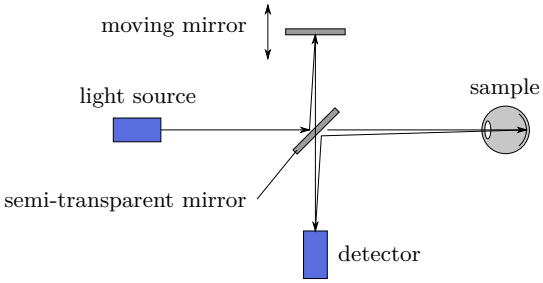

Figure 12.5: Setup of a time-domain OCT system, one mirror has been replaced with a sample. The other mirror can move to acquire an A-scan. The mirror is located in the reference arm, the sample in the sample arm.

Fig. 12.5). The remaining mirror M_1 forms part of the reference arm, whereas the sample becomes part of the sample arm. The sample has to be translucent enough to permit light to travel through it and to reflect back from different layers. Thus, movement of the mirror over time results in a depth profile of intensities of reflection at one position of the sample. This is called an A-scan. Directing the beam along a line across the sample, while acquiring A-scans at regular intervals, yields a two-dimensional image which is called a B-scan. Creating a raster scan of B-scans yields a volume. Every pixel column in Fig. 12.2 is an A-scan. The moving mirror is a disadvantage though, since it limits the maximum sampling speed of the OCT device.

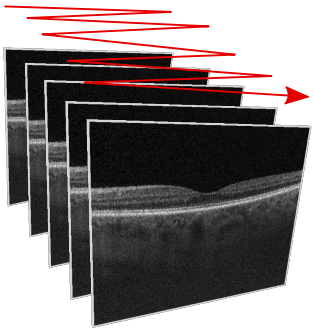

Figure 12.6: The OCT beam raster-scans the surface of the retina. Moving the beam along a line results in a B-scan (2-D image). Every column in a B-scan image is an A-scan. After each B-scan, the beam travels to the beginning of the next one.

12.3 Fourier Domain OCT

Modern Fourier domain OCT systems work differently. The spectrum of the A-scan can be acquired simultaneously and the moving mirror in the reference arm becomes unnecessary. Since we acquire the spectrum of the A-scan, we can apply an inverse Fourier-transform which yields the respective A-scan. This enables significantly higher acquisition speeds since the OCT device does not contain moving parts anymore.

Fourier domain OCT can be grouped into two variants. The first one is Spectral-domain OCT, where a spectrometer acquires the spectrum. The speed is limited by how fast the spectrometer can acquire the spectrum. Currently, resolutions of 3 µm with a scanning speed of up to 312.500 A-scans per second can be achieved.

The second one is swept-source OCT, where the light source sweeps across a spectrum and a detector samples the spectrum over time. The speed limit is set by how fast the light source can sweep across the spectrum, but the speed is generally higher than the speed of spectrometers used for Spectral-domain OCT. Resolutions of 5 µm while scanning 800.000 to 3.350.000 A-scans per second are currently possible in research systems.

12.4 OCT Angiography

OCT devices operate in the infrared light regime with wavelengths in the micrometer regime. Blood cells have diameters that lie in a similar range, i. e., white blood cells have diameters of 10–12 µm, red blood cells of 6–8 µm,

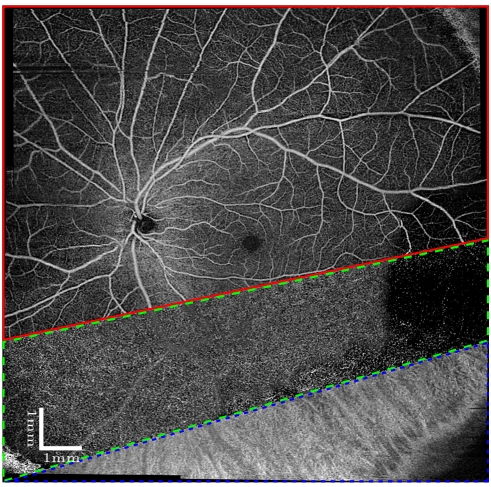

Figure 12.7: 3-D OCT angiography results in a layered reconstruction of the vessels for each retinal layer. Here we show a wide 12 mm × 12 mm field of view of the superficial and deep retina as well as the choroid (from top to bottom). Image data courtesy of New England Eye Center, USA.

and platelets of 2–3 µm. This size is just about right to induce high speckle noise in the image. In OCT angiography, this effect is exploited to create a visualization of vessels without the need of contrast agent. The idea is to scan the same area of the retina multiple times to generate a map of variance. This map will have a high response in areas that contain vessels. Using the structural OCT image (cf. Fig. 12.2), the retinal layers are then segmented and used to create projections of each layer. Fig. 12.7 shows such projections for the superficial and deep vascular plexi as well as the choroid. In Geek Box 12.2, we detail measures for OCT angiography reconstruction. Note that comparison of scans that were acquired in rapid sequence also allows for the estimation of blood flow speed. This topic is scope of current OCT research.

12.5 Applications

OCT is predominantly used for imaging the eye. However, its application is also quite common in other body regions. In the following, we summarize shortly OCT's fields of application.

- Ophthalmic Imaging: Retinal imaging is currently the major application for OCT. Both the retina and anterior eye can be imaged for diagnostic purposes completely non-invasively in 3-D. Furthermore, as described above, the vessel structure can also be investigated in 3-D without the use

Geek Box 12.2: OCT Angiography Signal Generation

In order to quantify the variance in OCT images, several measures have been proposed. *Speckle variance* assumes a normal distribution to compute the signal variance

$$\sigma^2_{\mathrm{SV}} = \frac{1}{N}\sum_{n=0}^{N-1}(I_n - \bar{I})^2 \tag{12.3}$$

where I_n are the individual structural measurements and $\bar{I}$ their corresponding mean value.
In order to accommodate the acquisition sequence, above concept can be expanded to only compare neighboring acquisitions. The resulting method is called *inter-frame variance*

$$\sigma^2_{\mathrm{IF}} = \frac{1}{N-1}\sum_{i=1}^{N-1}(I_{n-1} - I_n)^2 \tag{12.4}$$

Note that this measure again uses a normal distribution as underlying assumption. This time, however, we assume that the inter-frame differences are normally distributed and their mean is 0.
Another extension to this is the so-called *amplitude decorrelation* in which we introduce additional scaling to the variance computation.

$$\sigma^2_{\mathrm{AD}} = \frac{1}{N-1}\sum_{n=1}^{N-1}\frac{(I_{n-1} - I_n)^2}{I^2_{n-1} + I^2_n}. \tag{12.5}$$

This concept is very similar to inter-frame variance, however, a local scaling of $\sqrt{I^2_{n-1} + I^2_n}$ is introduced for every amplitude difference. Doing so, amplitude decorrelation is always scaled between 0 and 1 and therefore can be interpreted as an "inverse correlation" where 0 is obtained for correlated observations and 1 for independent measurements.

of contrast agent. As such, OCT has become the standard of care for the diagnosis of eye diseases. Fig. 12.8 shows a volume of the anterior eye and part of the retina.

- Cardiovascular Imaging: OCT can be used to diagnose cardiovascular diseases. In order to do so, optical fibers are embedded into a catheter that is inserted minimally invasively into the vessel system. Doing so, the vessel wall can be imaged and areas of concern can be investigated. These are typically calcifications and plaques that are attached to the vessel wall.

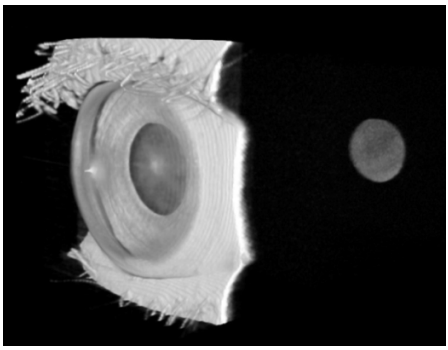

Figure 12.8: OCT volume showing the structure of the cornea, lens, and iris of the anterior eye. The disc in the background is part of the retina which is visible through the lens. These volumes are used in the visualization and diagnosis of corneal pathologies and glaucoma.

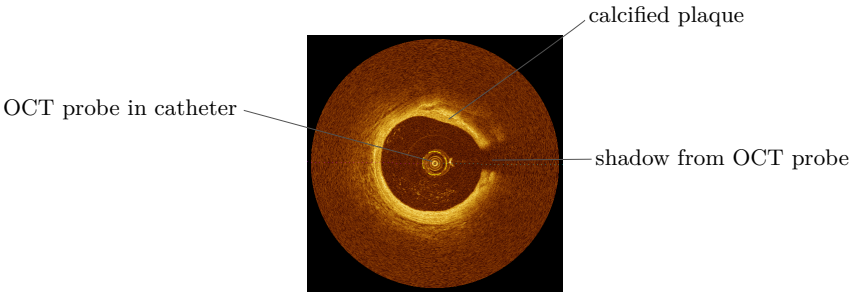

Figure 12.9: B-scan from a blood vessel. The small circle in the middle is the OCT probe within the dark lumen. The bright ring around the lumen is the vessel's endothelium (inner surface). The gap on the right side is caused by constructional properties of the probe. A calcified plaque is visible in the top right quadrant of the endothelium.

Fig. 12.9 shows a cross section of a blood vessel. A rotating mirror is mounted at the tip of the catheter and deflects the OCT beam into the tissue around the probe. OCT offers higher resolution when compared to intravascular ultrasound.

- Gastrointestinal Imaging: OCT is also used in gastrointestinal imaging, where it might have the potential to enable earlier detection and prevention of cancer. Current research investigates application in the esophagus and the colon.
- Dermatology: OCT angiography is investigated to detect skin cancer which has increased blood flow due to rapid growth of cancerous cells. Again, the combination of structural and functional imaging potentially can enable new ways of treatment. This topic is scope of current research.

Further Reading

[1] Bernhard Baumann et al. “Total retinal blood flow measurement with ultrahigh speed swept source/Fourier domain OCT”. In: *Biomedical Optics Express* 2.6 (2011), pp. 1539–1552. DOI: 10.1364/BOE.2.001539.

[2] Mark E Brezinski. *Optical coherence tomography: principles and applications*. Academic press, 2006.

[3] Emily Cole et al. “The definition, rationale, and effects of thresholding in OCT angiography”. In: *Ophthalmology Retina* 1/2017.5 (2017), pp. 435–447. DOI: 10.1016/j.oret.2017.01.019.

[4] Wolfgang Drexler and James G. Fujimoto. *Optical coherence tomography: technology and applications*. Springer, 2008.

[5] David Huang et al. “Optical Coherence Tomography”. In: *Science* 254.5035 (Nov. 1991), pp. 1178–1181. DOI: 10.1126/science.1957169.

[6] Martin Kraus et al. “Quantitative 3D-OCT motion correction with tilt and illumination correction, robust similarity measure and regularization”. In: *Biomedical Optics Express* 5.8 (2014), pp. 2591–2613.

[7] Jonathan J. Liu et al. “In vivo imaging of the rodent eye with swept source/Fourier domain OCT”. In: *Biomedical Optics Express* 4.2 (2013), pp. 351–363. DOI: 10.1364/BOE.4.000351.

[8] Markus Mayer et al. “Retinal Nerve Fiber Layer Segmentation on FD-OCT Scans of Normal Subjects and Glaucoma Patients”. In: *Biomedical Optics Express* 1.5 (2010), pp. 1358–1383.

[9] Stefan Ploner et al. “A Joint Probabilistic Model for Speckle Variance, Amplitude Decorrelation and Interframe Variance (IFV) Optical Coherence Tomography Angiography”. In: *Bildverarbeitung für die Medizin 2018*. Ed. by Andreas Maier et al. Informatik aktuell. Erlangen, 2018, pp. 98–102. ISBN: 3662565374. DOI: 10.1007/978-3-662-56537-7.

[10] Stefan Ploner et al. “Toward Quantitative Optical Coherence Tomography Angiography: Visualizing Blood Flow Speeds in Ocular Pathology Using Variable Interscan Time Analysis”. In: *Retina* 32 (2016). DOI: 10.1097/IAE.0000000000001328.

[11] Carl Rebhun et al. “Analyzing relative blood flow speeds in choroidal neovascularization using variable interscan time analysis OCT angiography”. In: *Ophthalmology Retina* 2.4 (2018), pp. 306–319. DOI: 10.1016/j.oret.2017.08.013.

[12] Franziska Schirrmacher et al. “QuaSI: Quantile Sparse Image Prior for Spatio-Temporal Denoising of Retinal OCT Data”. In: *Medical Image Computing and Computer-Assisted Intervention - MICCAI 2017, Proceedings, Part II*. Ed. by Maxime Descoteaux et al. Quebec City, QC, Canada, 2017, pp. 83–91.